





Rolling motion behavior of rockfall on gentle slope: an experimental approach

CUI Sheng-hua  <http://orcid.org/0000-0002-6638-230X>; e-mail: shenghuacui.geo@gmail.com

PEI Xiang-jun*  <http://orcid.org/0000-0003-0790-4099>;  e-mail: peixj0119@tom.com

HUANG Run-qiu  <http://orcid.org/0000-0003-2560-4962>; e-mail: hrq@cdut.edu.cn

* Corresponding author

State Key Laboratory of Geohazard Prevention and Geoenvironment Protection, Chengdu University of Technology, Chengdu 610059, China

Citation: Cui SH, Pei XJ, Huang RQ (2017) Rolling motion behavior of rockfall on gentle slope: an experimental approach. *Journal of Mountain Science* 14(8). DOI: 10.1007/s11629-016-4144-7

© Science Press and Institute of Mountain Hazards and Environment, CAS and Springer-Verlag Berlin Heidelberg 2017

Abstract: The effects of slope surface material, slope gradient, block shape, and block mass conditions on rockfall rolling velocity were estimated with orthogonal test approach. Visual analysis shows that the importance of the factors is slope surface material > slope gradient > block shape > block mass. All the factors except block mass have the F value greater than the critical value, suggesting that these three factors are the key factors affecting the rockfall rolling velocity. Factor interaction analysis shows that the effect of the slope gradient relies largely on the slope surface conditions, and the block shape has little influence if the slope gradient is larger than a critical value. An empirical model considering the three key factors is proposed to estimate the rolling velocity, of which the error is limited to 5% of the testing value. This model is validated by 73 field tests, and the prediction shows excellent correlation with the site test. Thus, this analysis can be used as a tool in the rockfall behavior analysis.

Keywords: Rockfall; Rolling motion; Experiment approach; Gentle slope; Orthogonal test

Introduction

A huge amount of the rockfalls that led to the

damage of infrastructure and death of people have been reported all over the world (e.g., [Guzzetti et al. 2003](#); [Pellicani et al. 2016](#)). Rockfall hazards have become a major risk in the mountainous areas that endanger human lives and properties, especially after the 2008 Wenchuan earthquake, China.

The physical and chemical weathering are environmental activities that contribute to the development of the rockfall ([Jaboyedoff et al. 2004](#)). Slope morphology is an essential component in determining rockfall occurrence and movement ([Jomelli and Francou 2000](#)). Rainstorm ([Chau et al. 2003](#)), the frost-thaw activities ([Perret and Kienholz 2004](#)), seismic activities ([Saroglou et al. 2012](#)), human and animal activities ([Selby 1982](#); [Apostolou et al. 2015](#)) are the contributing factors. The information of the block velocity, jump height, run-out zone, and trajectory is the basis for the creation of accurate design and the verification of protective measures ([Dorren 2003](#); [Volkwein et al. 2011](#)).

The statistical methods ([Zvelebil and Moser 2001](#)), hazard inventories ([Evans and Hungr 1993](#); [Bull et al. 1994](#)), and mathematical formulas such as kinematics, elastic-plastic mechanics, tribology and elastic collision theory were widely used in the study of rockfall. The empirical models ([Piacentini and Soldati 2008](#); [Copons et al. 2009](#)),

Received: 28 July 2016
Revised: 12 September 2016
Accepted: 10 February 2017

process-based models (Evans and Hungr 1993; Chen et al. 1994; Asteriou et al. 2016), GIS-based models, Lidar-based models (Dorren and Seijmonsbergen 2003; Lan et al. 2007; Lan et al. 2010), and Terrestrial Laser Scanner models (Abellán et al. 2006) were established for calculating the run-out zone and trajectory of rockfall.

The numerical models were widely used, including distinct element method (DEM), discontinuous deformation analysis (DDA) and other related codes (such as STONE and ROCKFALL programs), varying from 2D to 3D models (Crosta and Agliardi 2004; Jaboyedoff et al. 2005; Wang et al. 2011; Chen et al. 2013; Thoeni et al. 2014). The dynamic effects of three dimension topography were ignored in 2-D model. Thus, pseudo 3-D assumptions (Jaboyedoff et al. 2005) were introduced to overcome this limitation partly. Full 3D numerical modeling had been presented to do lateral dispersion of 3D trajectories and the related effects on probability and intensity assessment (Crosta and Agliardi 2004; Thoeni et al. 2014). Lumped mass method and rigid body method were involved in numerical simulations (Basson 2012; Bourrier et al. 2012). The former method ignored the block geometry and scale, so the block mass had no effect on rockfall motion except energies. And in the rigid body method, the interaction investigation between the block and slope surface is possible.

Researchers performed out-field experiments to estimate the rockfall motion by throwing different types of rock blocks and monitoring their moving velocity (Kirkby and Statham 1975; Okura et al. 2000; Giani et al. 2004; Dorren et al. 2006), but these were time- and labor-consuming. The laboratory test combined with the mathematical model was effective in investigating the rockfall motion (Fan et al. 2016). This method had been widely used in the study of the rockfall impact motion (Chau et al. 1999; Chau et al. 2002; Asteriou et al. 2012; Asteriou et al. 2016). However, these kinds of study of the rockfall rolling motion were limited.

The factors that affecting the rockfall rolling motion are slope geometry, local roughness of slope, and the interactions between the slope features and the block dynamics during bouncing, sliding, and rolling (Crosta and Agliardi 2004). In

this study, orthogonal experiment method was used to design test program in the laboratory. A series of rockfall tests were conducted on a gentle slope.

1 Field Observations

Rockfall has been a serious threat to human lives and properties in the earthquake area of the 2008 Wenchuan earthquake, China (Pei et al. 2011; Pei et al. 2016). Upon investigation, the most common materials covering the rockfall slope surface were soil, bedrock, and scree (Figure 1). The rock blocks stop at the foot of the slope and the slope surface. Some blocks were even located at the toe of the source area (Figure 2a). There are different block shape types such as cubic-like, cuboid-like, and spherical-like block (Figure 2b). Some rockfall hazards involving huge rock blocks led to severe damages (Figure 2c). During the earthquake, the rockfall-induced damages to the tunnels, bridges, and roads were very significant (Figure 3). According to the traces on the slope surfaces, falling, bouncing, and rolling motions were observed as the major rockfall motions. The rock blocks were gradually initiated with the falling motion due to the steep profile of the source area. The bouncing rock blocks after colliding on the slope surface gradually shifted their rolling motions due to rapid rotational momentum. Although there were different slope profiles with different gradients, a portion of them were composed of straight segment with gentle gradient. The rolling motion on the gentle straight slope can be observed frequently.

2 Methods

2.1 Laboratory tests

A flat, inclined ramp slope model was built with 0.3 m in width and 2.45 m in length. The endpoint of the slope was fixed. The slope gradient can be adjusted by changing the height of the initial point (Figure 4), and will affect the rockfall motion after the rock has been released. According to Ritchie (1963), the motion of rock block would be bounced if the slope gradient was more than 45°. As the gradient reached the 70° or more, the rock

block would gradually transform from bouncing to falling. A bouncing block changed its motion to rolling due to the rotational momentum when the slope gradient was less than 45° . The sliding occurred gradually in the final stage on a very gentle slope. The sliding rock block stopped because of the friction force. In order to investigate the rolling motion of the rock block, the gentle gradients that ranged from 18° to 30° were chosen for the lab tests in this study.

The geometry of a rock block was an essential factor that affects its rolling motion (Fityus et al. 2013; Fityus et al. 2015). Three shape forms such

as spherical (SP1), cubic (SP2), and cuboid (SP3) were chosen in this study. The blocks were made of the same concrete material with quite rough surfaces based on the roughness and irregular properties of rockfall block in the field. The rock blocks of each type had three different weights: 1 kg, 2 kg, and 3 kg (Figure 5). The blocks were regarded as rigid body with no fracture, and did not break up during the test. The diameters of the SP1 ranged from 4.62 cm to 6.66 cm. The side lengths of the SP2 were ranging from 7.5 cm to 10.7 cm. For the SP3, the principal side length ranged from 6.1 cm to 8.8 cm and short ones got half of the length.

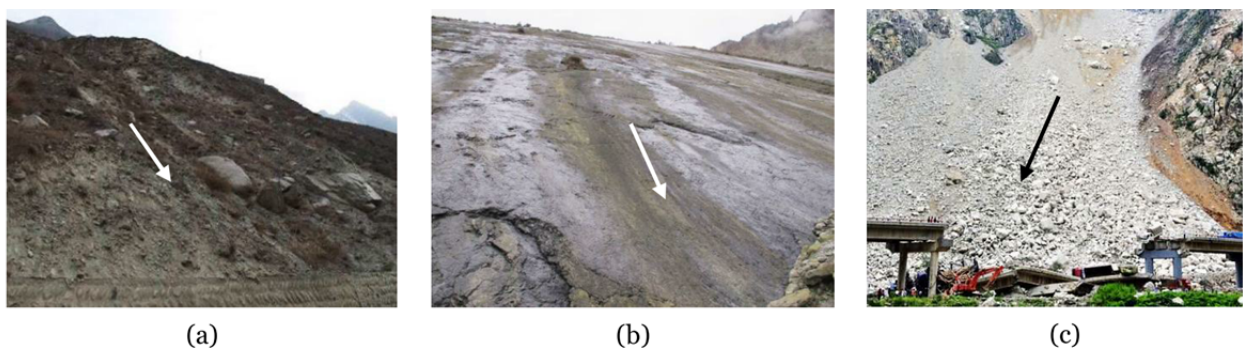


Figure 1 Slope surface material. (a) Soil slope surface, (b) bedrock slope surface, (c) scree slope surface.

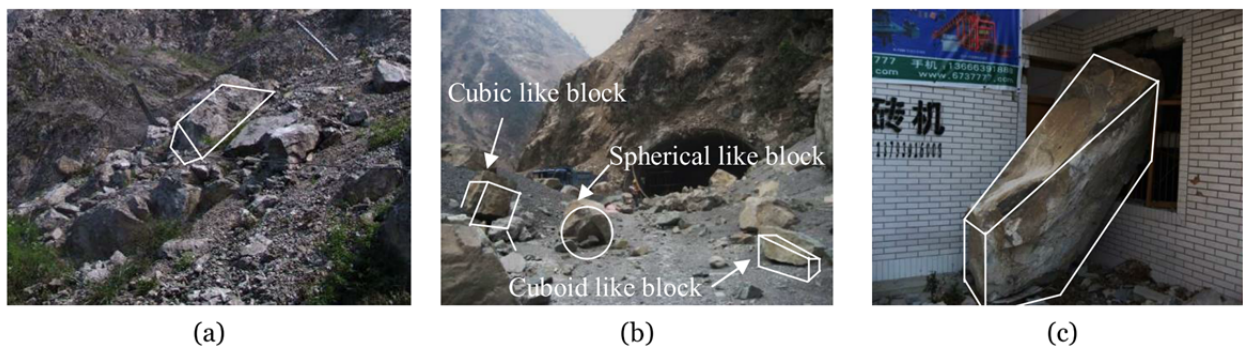


Figure 2 Stop position and shape of the rock block. (a) Blocks stop on the slope surface, (b) cubic like, spherical like and cuboid like block stopping at the foot of the slope, (c) huge rock block.

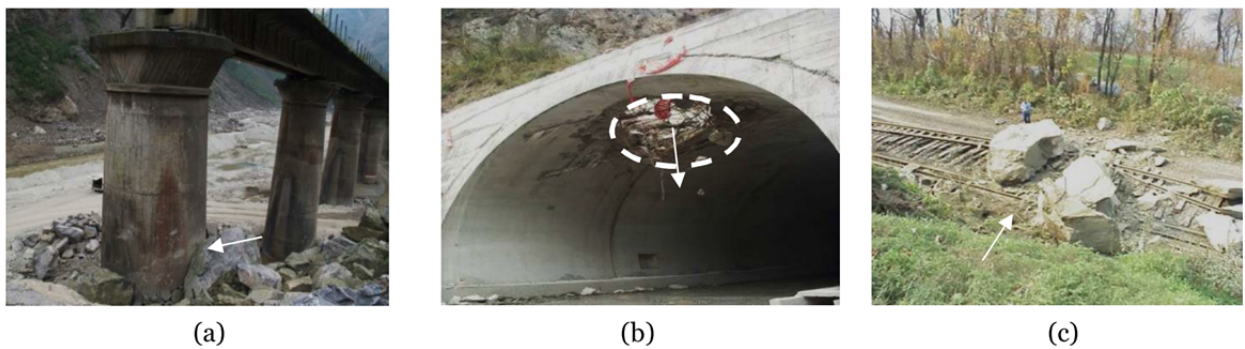


Figure 3 Rockfall hazards. (a) To bridge, (b) to tunnel, (c) to railway.

The rock blocks moved on the slope surface after released. The slope surface material would make a difference to their rolling motion. Based on our field investigations and the previous studies (Chau 2002; Paronuzzi 2009), three types of slope surface materials such as bedrock, scree, and soil were used in tests. The hard bedrock was simulated by the board (M1). The soil material with a density of 2.05 g/cm³ and water content of 7 % (M2) was composed of clay and gravel. The dry gravel material with certain grading was used to simulate the scree (M3). The coefficients of uniformity ($C_u = d_{60}/d_{10}$) of M2 and M3 were 13.7 and 2.5, respectively and the coefficients of curvature ($C_c = d_{30}^2 / (d_{60} \times d_{10})$) were 2.3 and 3.9, respectively (Figure 6).

The orthogonal test method was employed for designing the test program (Table 1). An additional column E (Error column) in the orthogonal table was added for variance analysis. So the $L_{27}(3^5)$ orthogonal table was chose, which meant there were 3 levels for one factor, 5 columns in the table and 27 tests were required in total (Table 2). Firstly, the slope model was placed horizontally and the surface material was set on the slope surface uniformly with a thickness of 10 cm except the M1. Then the slope model was set to a certain gradient by increasing the height of the initial point. The rolling behavior of block was heavily dependent initial condition (Fityus et al. 2013), so it was necessary to release the block in a representative way. In the test, all blocks were released from the resting positions at the top of the ramp by hand. Before initiation, the spherical blocks needed to contact the slope surface (Figure 7a); the cubic blocks were placed on an edge with an orientation of the rolling onto faces in their first motion (Figure 7b) and the cuboid blocks were stood by with a maximum edge and rolled onto faces in their first motion (Figure 7c). The diagonals of the cross-sections of the SP2 and SP3 were parallel to the slope surface

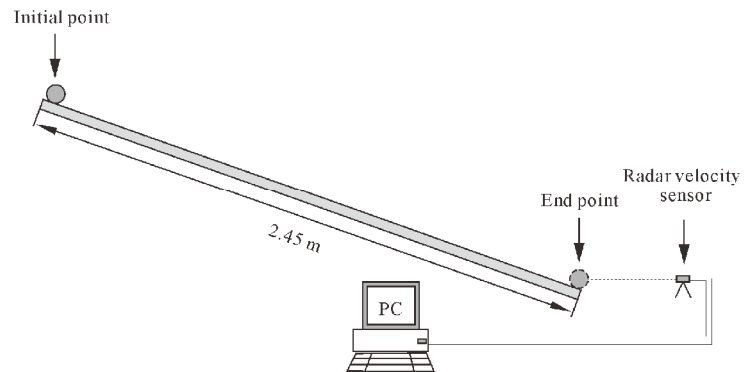


Figure 4 Experiment set-up in State Key Laboratory of Geohazard Prevention and Geoenvironment Protection (SKLGP).

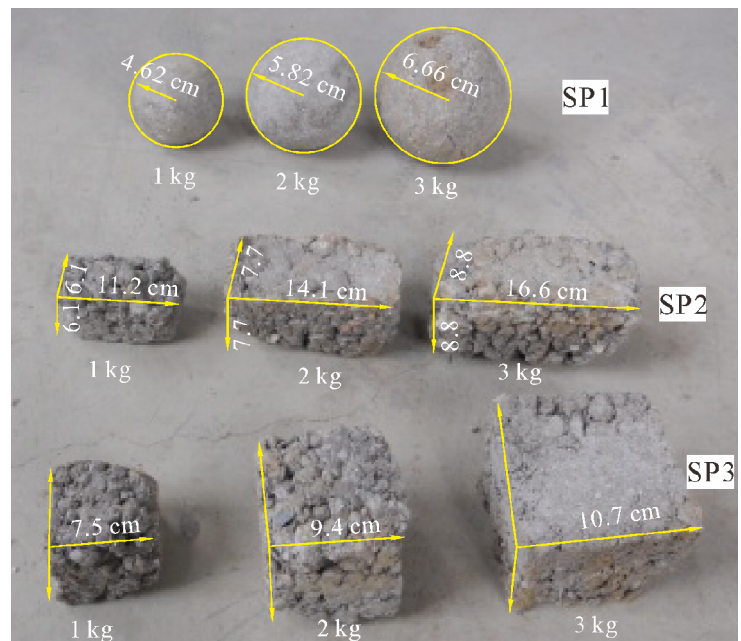


Figure 5 Spherical (SP1), cubic (SP2) and cuboid (SP3) samples, which were made of the same concrete material with quite rough surfaces due to the roughness and irregular properties of the rockfall block in the field.

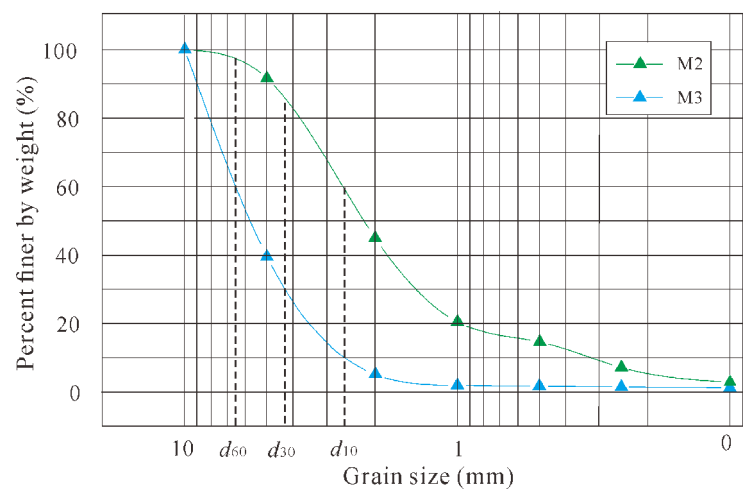


Figure 6 Grain-size distributions.

when they were initiated.

The CRLK type radar made in America was used to measure the block velocity at the endpoint of the slope model. It had a measurement accuracy of 0.01 m/s. The tests were conducted referencing the test list in the orthogonal table (Table 2). The tests might be disturbed when the block impacted on the side walls due to the limited width of the ramp model. These blocks would lose a big portion of kinetic energy and might be ceased rapidly before reaching the endpoint. These tests were conducted again and the results of these tests were not used. For each test number, five parallel tests were conducted and the average value was regarded as the final value excluding the bad tests.

2.2 Methods for modeling

In previous studies, the rock block that described as a ball or ellipse form (Labieuse and Heidenreich 2009; Chang et al. 2011; Wang and Tonon 2011). Azzoni and de Freitas (1995) gave a common denotation as the ratio between the volume of the block and the minimum sphere included within the block. Based on this concept, two parameters d_c and d_{cy} are defined:

$$d_c = V_r / V_c \tag{1}$$

$$d_{cy} = V_r / V_{cy} \tag{2}$$

where, V_r is the volume of rock block, V_c is the minimum sphere volume that can accommodate the block if it is a cubic or sphere, V_{cy} is the minimum cylinder volume that contains a rock block if that block is like a cuboid. Parameter $\lambda = l_{min}/l_{max}$ is defined, where l_{max} is the maximum length of the block, l_{min} is the minimum length of the block. The rock block was identified as a sphere-like block when $\lambda > 0.5$ and the Eq.(2) was chose for calculation. If not, the Eq.(1) was used.

If a rock block moved in contact with the slope surface with no sliding arising, the friction force acting on the block was defined as a rolling friction (Kirkby and Statham 1975). The rolling motion was composed of a succession of small bounces when the block hit the slope surface with the roughness scales. The process still could be described as rolling with a steady velocity if the block

Table 1 Factors and levels of the orthogonal test

| Levels | Factors | | | |
|---------|---------|---|-----|----|
| | A | B | C | D |
| Level 1 | M1 | 1 | SP1 | 18 |
| Level 2 | M2 | 2 | SP2 | 24 |
| Level 3 | M3 | 3 | SP3 | 30 |

Table 2 Orthogonal tests showing the factors and testing velocity value

| Number | A | B | C | D | E | v_n |
|----------|-------|-------|-------|-------|-------|--|
| 1 | 0.25 | 2 | 1 | 18 | E1 | 2.93 |
| 2 | 0.25 | 2 | 0.37 | 24 | E2 | 2.91 |
| 3 | 0.25 | 2 | 0.28 | 30 | E3 | 2.83 |
| 4 | 0.25 | 3 | 1 | 24 | E3 | 3.33 |
| 5 | 0.25 | 3 | 0.37 | 30 | E1 | 3.33 |
| 6 | 0.25 | 3 | 0.28 | 18 | E2 | 2.45 |
| 7 | 0.25 | 1 | 1 | 30 | E2 | 3.27 |
| 8 | 0.25 | 1 | 0.37 | 18 | E3 | 1.70 |
| 9 | 0.25 | 1 | 0.28 | 24 | E1 | 2.74 |
| 10 | 0.31 | 2 | 1 | 24 | E1 | 2.86 |
| 11 | 0.31 | 2 | 0.37 | 30 | E2 | 2.49 |
| 12 | 0.31 | 2 | 0.28 | 18 | E3 | 1.60 |
| 13 | 0.31 | 3 | 1 | 30 | E3 | 2.87 |
| 14 | 0.31 | 3 | 0.37 | 18 | E1 | 1.70 |
| 15 | 0.31 | 3 | 0.28 | 24 | E2 | 2.36 |
| 16 | 0.31 | 1 | 1 | 18 | E2 | 2.76 |
| 17 | 0.31 | 1 | 0.37 | 24 | E3 | 2.27 |
| 18 | 0.31 | 1 | 0.28 | 30 | E1 | 2.72 |
| 19 | 0.38 | 2 | 1 | 30 | E1 | 2.18 |
| 20 | 0.38 | 2 | 0.37 | 18 | E2 | 1.45 |
| 21 | 0.38 | 2 | 0.28 | 24 | E3 | 1.75 |
| 22 | 0.38 | 3 | 1 | 18 | E3 | 1.73 |
| 23 | 0.38 | 3 | 0.37 | 24 | E1 | 1.76 |
| 24 | 0.38 | 3 | 0.28 | 30 | E2 | 2.34 |
| 25 | 0.38 | 1 | 1 | 24 | E2 | 2.21 |
| 26 | 0.38 | 1 | 0.37 | 30 | E3 | 2.44 |
| 27 | 0.38 | 1 | 0.28 | 18 | E1 | 1.15 |
| S_{ij} | 25.47 | 21.06 | 24.12 | 17.46 | 21.33 | $v = \sum_{n=1}^{27} v_n$ $= 64.14$ $\bar{v} = 2.38$ |
| S_{2j} | 21.6 | 21.87 | 20.07 | 22.23 | 21.60 | |
| S_{3j} | 17.01 | 21.24 | 19.98 | 24.48 | 13.14 | |
| K_{ij} | 2.83 | 2.34 | 2.68 | 1.94 | 2.37 | |
| K_{2j} | 2.40 | 2.43 | 2.23 | 2.47 | 2.40 | |
| K_{3j} | 1.89 | 2.36 | 2.22 | 2.72 | 1.46 | |
| R | 0.94 | 0.09 | 0.47 | 0.78 | 0.94 | |

dimensions were much greater than the roughness lengths (Bozzolo and Pamini 1986; Dorren 2003). The rolling motion could be described using the Coulomb's law of friction which relied both on the slope surface materials and the ratio between the block diameter and the slope partial size. The following model denoted by Kirkby and Statham (1975) was used in this study,

$$f_{ud} = \tan\Phi_o + k \times (d_u/D_u) \quad (3)$$

where, f_{ud} is the tangent value of synthesis friction angle Φ_{ud} , Φ_o is the angle of internal friction, d_u is the partial size on the slope, D_u is the diameter of the rock block, k is the constant between 0.17 and 0.26 (Kirkby and Statham 1975).

The λ value of SP1 and SP2 were larger than 0.5 and of SP3 was smaller than 0.5. The calculated shape coefficients of SP1, SP2, and SP3 were 1, 0.37 and 0.28, respectively. The $\Phi_o = 27^\circ$ and $k = 0.2$. The calculated slope surface coefficients of M1, M2, and M3 were 0.25, 0.31 and 0.38, respectively. The slope gradient was transformed into a non-dimensional factor by dividing by 90° . The detailed testing program was shown in the orthogonal table (Table 2). After testing, the velocity data was used to fit a regressing model against the chosen factors.

3 Results

3.1 Motion features

The small jumps and slips which were connected to the momentum occurred when the blocks were prevented by the slope irregularities (Figure 8a) as described by Azzoni (1995). The blocks bouncing up impacted on the slope surface with kinetic energy loss. The cubic and cuboid blocks were easier to roll over the barriers than the sphere blocks. The main reason was that their dimensions were larger than the roughness size; they could roll steadily over the contact points. The slope surface material generated non-linear deformations because of the rolling motion (Figures 8b and 8c), which resulted in the increase of the resistance force.

The rolling motion of the sphere block was steady in almost one consistent direction while the cubic and cuboid blocks were more intense. For the cubic blocks, as the length of edge was the same, the rolling along the edges resulted in less kinetic energy loss (Figure 8e). But this type of motion was sensitive to the large obstructions which would change their motions easily to a side-face type (Figure 8d). The cuboid blocks rolled approximately on their longest dimensions, but they were also sensitive to the large obstructions which would lead them to cease rapidly due to their

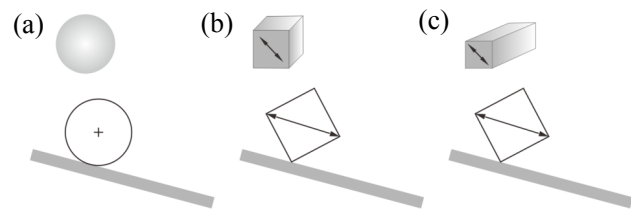


Figure 7 Release positions of each block sample type.

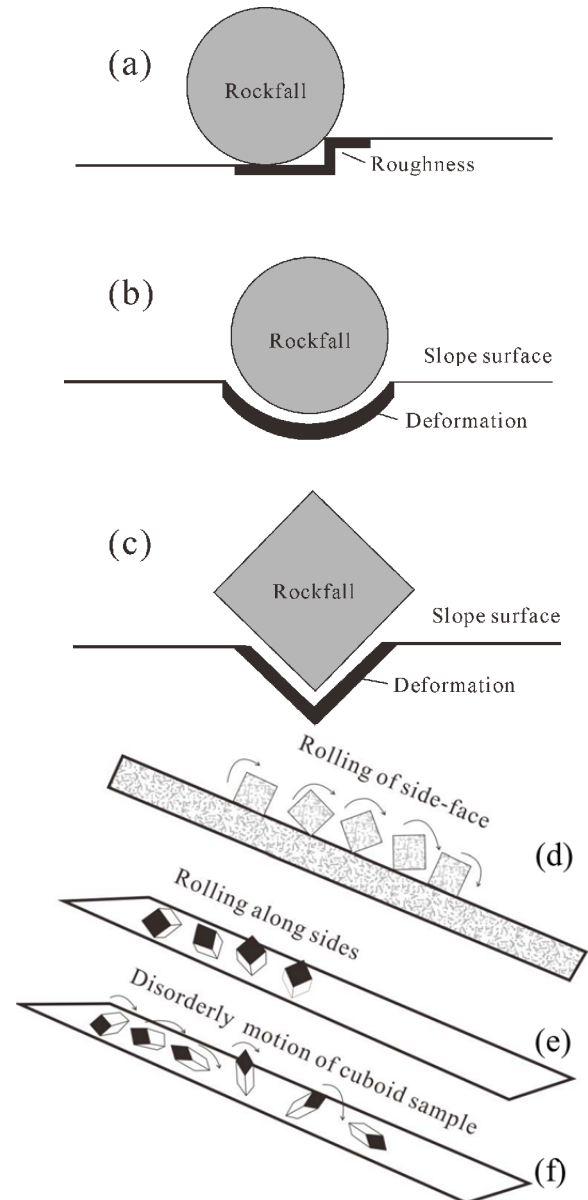


Figure 8 Description of tests. (a) Influence of roughness of the slope surface, (b) and (c) influence of deformation of the slope surface (d) rolling type of edge to face, (e) rolling along edges, (f) disorderly motion of SP3.

longest axis were normal to the slope surface (Figure 8f).

3.2 Visual analysis result

The measured data was shown in Table 2. S_{ij} was the sum of the velocities of the level i ($i = 1, 2, 3$) for the factor j ($j = A, B, C, D, E$). K_{ij} was the average of the sum. S_{ij} represented the contributions of the level i and the factor j to the rolling. Y was the sum of the velocities from 1 to n ($n = 27$). The results were plot by factors as X-axis, K_{ij} as Y-axis (Figure 9). The Y-axis values decreased rapidly with the changes in the slope surface materials from M1 to M3. The Y-axis values increased rapidly with the increasing slope gradient. The changes of block shape form from SP1 to SP3 caused greatly decline of the Y-axis values, but the differences of the Y-axis values were negligible with the block shape changing from SP2 to SP3. The Y-axis values did not have much difference with the changes of block weight.

For factor j , the difference of the K_{ij} value means the effect of the factor j on the rockfall rolling velocity. The R was calculated by the following equation to do significance analysis of the factors.

$$R = \max(K_{ij}) - \min(K_{ij}) \quad (4)$$

The results of factors A, B, C and D were 0.94, 0.09, 0.47 and 0.78, respectively (Table 2). It indicated that the slope surface material has the greatest influence on the block rolling velocity while the block weight has the minimum. The importance of the factors affecting the rolling velocity was the slope surface material > slope gradient > block shape form > block mass.

The results of variance analysis are shown in Table 3. Firstly, $P = \frac{1}{n}Y^2$ and $S_A = \frac{\sum y_i^2}{9} - P$ were calculated. Where, y_i is the velocity of the level i of the factor A. Similarly, S_B, S_C, S_D, S_E for factor B, C, D and E could be calculated. And then the degree of freedom of each factor and freedom degree of the error (column E) was calculated. Then the mean deviation was calculated, which was the ratio of the sum of squares of deviations (S_B, S_C, S_D or S_E) to the freedom. Finally, the F value was calculated, which was the ratio of the sum of squares of mean deviations to that of the error. The details were shown in Table 3. The slope surface got the maximal F value and the block weight got the minimum that the trend was similar to the R analysis as stated previous. The F value of slope surface material, block shape, and slope gradient were greater than the critical values (95% confidence interval) except the block mass. It suggested that the block weight was a negligible

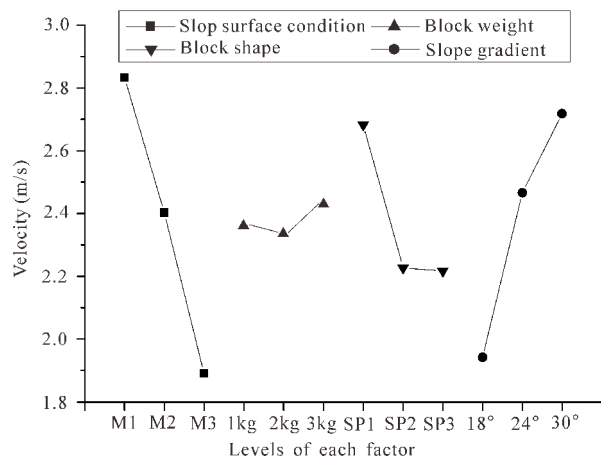


Figure 9 Visual analysis for the levels of the each factor.

Table 3 Results of orthogonal variance analysis

| Factors | S | df | S/df | F value | Critical value |
|---------|------|----|--------|---------|---------------------------|
| A | 4.01 | 2 | 2.00 | 224.7 | $F_{0.01}(2,18)$ =6.01 |
| B | 0.04 | 2 | 0.02 | 2.4 | |
| C | 1.27 | 2 | 0.64 | 71.9 | |
| D | 2.82 | 2 | 1.41 | 158.4 | $F_{0.05}(2,18)$ =3.35 |
| E | 0.16 | 18 | 0.0089 | -- | |

Notes: Notes: A: Slope surface material; B: Sample weight (kg); C: Sample shape; D: Slope gradient (°); E: Error column; S: Sum of squares of deviations; Df: Degree of freedom; S/df: Mean square.

factor. So, the block weight was excluded in the following analysis.

3.3 Interaction of the factors

Figure 10a showed the interaction of the slope surface material (rolling friction coefficient) and the block shape coefficient to the rockfall rolling velocity which ranges from 1.75 m/s to 3.18 m/s. The rolling velocity decreased with increasing rolling friction coefficient in the same block shape form and with decreasing shape coefficient under the same surface condition. The rolling velocities almost did not change when the block shape coefficient changing from 0.28 (cuboid) to 0.37 (cubic) in the same slope surface condition until the block shape coefficient changed from 0.37 to 1 (spherical). Figure 10b showed the interaction of the block shape form and slope gradient to the rolling velocity that the value was in the range of 1.73 to 2.77 m/s. The rolling velocity increased with the slope gradient arising, but the extent of changing decreased with the slope gradient increasing. The velocity almost didn't change as the

block shape coefficient changed under the 30° slope gradient condition. It could be noted that the effect of the block shape form was little on the rockfall rolling velocity after the slope gradient was larger than the critical value. Figure 10c illustrated

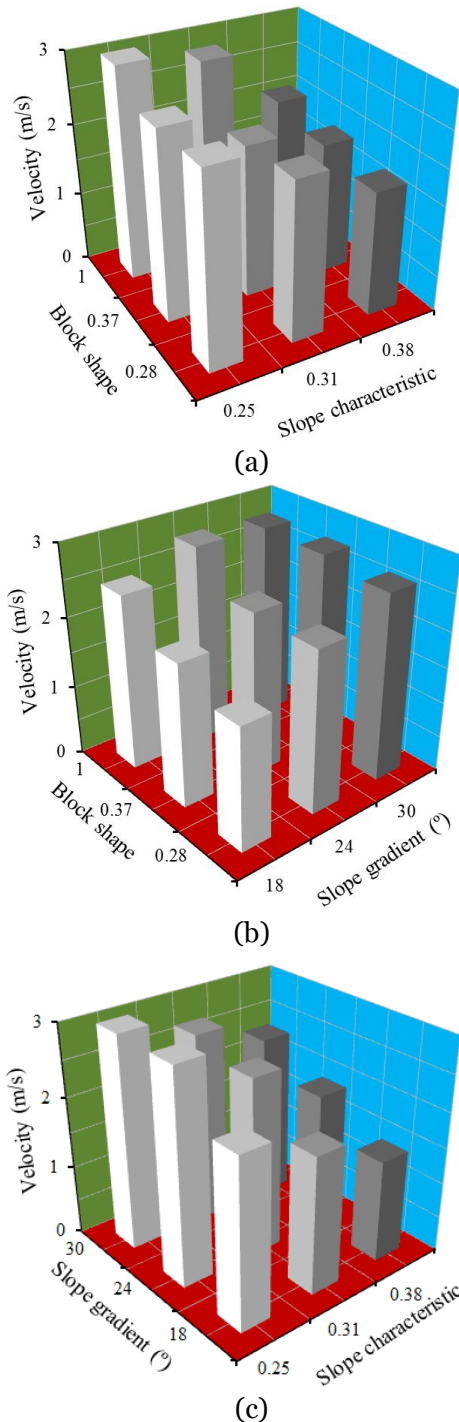


Figure 10 Interaction analyses. (a) Interaction between block shape and slope surface material, (b) Interaction between block shape and slope gradient, (c) Interaction between slope gradient and slope surface material.

the interaction of the slope gradient and the slope surface material to the rockfall rolling velocity where the value was in the range of 1.44~3.14 m/s. The velocity increased as the slope gradient increasing under the same slope surface material condition. The velocities stay stable as the slope gradient changing from 24° to 30° under the 0.25 slope surface coefficient condition. It indicated that the effects of the slope gradient on the rockfall rolling velocity relied largely on the slope surface conditions.

3.4 Modeling of the rolling velocity

A regression model $v_c = a_1X_1^{a_2} + a_3X_2^{a_4} + a_5X_3^{a_6}$ is used to build a simple rolling velocity relationship based on the testing data, where X_1 , X_2 , and X_3 are the rolling friction coefficient, block shape coefficient, and non-dimensional slope gradient, a_1 to a_6 are the fitting parameters. The proposed model is denoted as follows:

$$v_c = -7.84X_1^{0.54} + 0.47X_2^{3.2} + 8.79X_3^{0.24} \quad (5)$$

To ensure that the proposed model procedure was consistent with the experimental results, a comparison between the measured velocities and the calculated velocities from the empirical model was presented (Figure 11). The error of the estimating value was limited to 5% of the testing value. It became evident that the model predictions were in a very good correlation with the experimental results. Considering the variation of slope length (L) and the initial velocity (v_0), a simplified Eq.6 was given where 2.45 in meter was the slope length in our laboratory test. The model was further verified with field data as presented in the following section.

$$v = v_0 + \frac{L}{2.45} v_c \quad (6)$$

4 Model Verification

In order to evaluate the potential applicability for estimating the rockfall rolling velocity of the proposed model derived from laboratory experiments, field tests were conducted in a Mountain located in Mianning County, China (Huang et al. 2007). This site had numerous large limestone blocks. The dropping blocks with rough surface were shaped to the specimens like which

used in the laboratory tests. The maximum dimension equaled to 50 cm. The slope with total length of 62.8 m was composed of two segments. The upper segment from point A to point C has a length of 30.2 m and slope gradient of 40° (Figure 12). The surface material was dense soil. The lower segment from point C to D has length of 32.6 m and slope gradient of 35°. The surface material was gravel. The rolling friction coefficient, the block shape coefficient, and the non-dimensional slope gradient of rock blocks were calculated using the methods proposed in this study. The rock blocks were initiated by hand with no initial translation and rotation velocities at the upper position (Point A), middle position (Point B) and lower position (Point C) respectively as shown in Figure 12. The final translation velocity of the rock block was recorded by the radar velocity sensor at the foot of the slope (Point D). 73 in situ tests were executed in total. The rolling velocities were estimated using the proposed Eq.(6). For trajectory A-D or B-D, the rolling velocity at point C was calculated firstly by using Eq.(6); and then, this velocity was used as the initial velocity to calculate the rolling velocity at point D by using Eq.(6) again. The estimated data was used to do comparison with the field data for verifying the proposed model.

The results of the three different initial points were shown in the three columns respectively (Figure 13). The testing and estimating data were shown as solid and hollow mark, respectively. For segment C-D and B-D, it can be found that most of the estimation value lay under the 10% error boundary of the testing value, which suggests the validity of the proposed model in this study. It indicated that the rolling velocity model derived from the laboratory tests could describe the rolling movement of the blocks in the field site. However, the estimated velocities of A-D segment had about 30% positive errors which will be

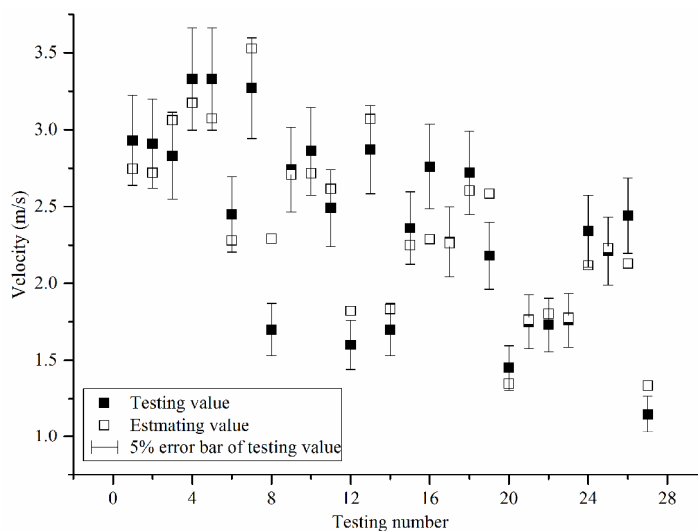


Figure 11 Comparison between the lab testing value with 5% error line and the estimating value.

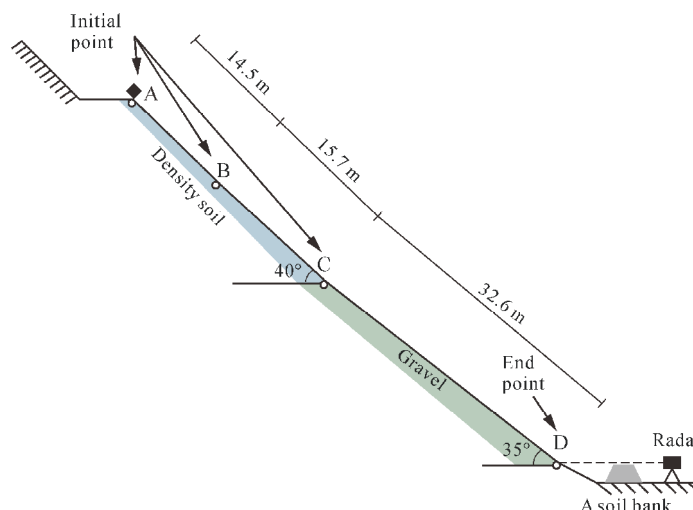


Figure 12 Slope model of the field tests.

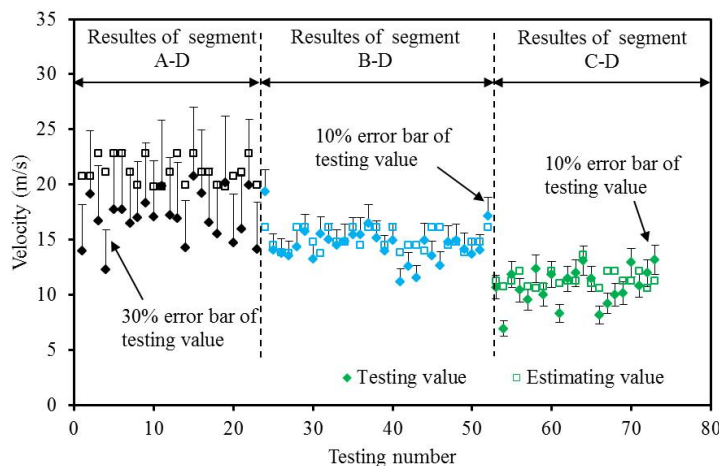


Figure 13 Comparison between the field data and the estimating value.

discussed later.

5 Discussions

Describing the shape of the rockfall is quite difficult because that there are numerous possible rock fragments in the field. Some researchers used several simple geometrical shapes to conduct rockfall motion research, such as sphere, cylinder, cubes, ellipse, and circle forms (Chau et al. 1999; Chang et al. 2011). To investigate the relationship between block geometry and the rockfall motion, Fityus et al. (2013) defined a series of basic forms that were classified into basic ball forms, cylinder forms, cone forms, disc forms, and acute forms from categories by defining three principal dimensions. However, the quantitative description of the rockfall geometry was limited in these studies. For quantification, Azzoni and de Freitas (1995) provided a rough denotation for all blocks based on geometry. Vijayakumar et al. (1996) used a mathematical method to calculate the shape coefficient. Although more complicated block shapes can be described by a Fourier series, it was just a 2D model by ignoring space effect. In this study, we tried to do a quantitative description for a rock block. A method of quantitative description of the sphere, cubic and cuboid was proposed. The sphere or cubic block were more similar to ball and cuboid was more similar to cylinder. The ratio between the block volume and the minimum sphere volume within the block was used to describe the shape of the sphere or cubic block. The ratio between the block volume and the minimum cylinder volume within the block was used to describe the shape of the cuboid block. This definition might be more effective than that proposed by Azzoni and de Freitas (1995).

Fityus et al. (2015) noted the effect of the shape on the inherent rolling potential of the rock block in the laboratory. The results showed that the sphere blocks were more prone to roll and their tendency to roll was strongly influenced by the number of phases. In this study, the same features were revealed, i.e., the rolling velocities almost did not change when the block shape changing from cuboid to cubic until it changing to spherical. It was also found that the difference in length of block edge also had important influence on rockfall rolling motion. Azzoni and de Freitas (1995) found

relationship between the rolling velocities and the block shape coefficient, which was ascribed to the small block size ($< 0.4 \text{ m}^3$). The little velocity difference between the cubic and the cuboid blocks (Figure 9) might be also ascribed to the reason that block size was small in this study. The block mass has the most significant influence on the rolling velocity in this study. It was reasonable and was one of the reasons that the lumped mass models were commonly used in many studies. But both the block volume and dimension were found related to the rolling velocity (Azzoni and de Freitas 1995; Vijayakumar et al. 1996; Glover et al. 2012; Fityus et al. 2013; Leine et al. 2014). These factors were limited in our tests because of the insufficient equipment. These limitations could probably be overcome in large-scale situ tests.

Slope surface conditions could greatly vary in a short distance in the field, i.e., a slope might be consisted of several surface materials. The slope surface materials involved in this study were widely used in the laboratory and field tests of the other studies (Evans and Hungr 1993; Sass and Krautblatter 2007; Asteriou et al. 2012; Dorren et al. 2016). Although initial conditions of the rockfall were constant, the trajectories of the blocks on the slope could vary a lot (Azzoni and de Freitas 1995). So the dynamic angle of friction was generally used to investigate the effects of the rolling motion of rockfall. The dynamic friction force was the interaction between the deformation of the materials and the ratio between the block size and the roughness scales. This idea was also used to describe the slope surface condition in this study. The frictional force is the reason of kinetic energy losing during the rockfall movement. The Coulomb's law of friction was generally used to calculate the rolling and sliding velocities:

$$F_f = \mu_f \times m \times g \times \cos\beta \quad (7)$$

where F_f is friction force, μ_f is coefficient of friction, m is mass of the rock, β is mean slope gradient. Hence, the friction coefficient and slope gradient were important factors (Dorren 2003) and widely used for measuring the rockfall velocity (Okura et al. 2000; Giani et al. 2004; Paronuzzi 2009; Leine et al. 2014; Ferrari et al. 2016). The friction coefficient relied on material type, block shape, and slope gradient as known. But the study of their interaction on the rolling velocity of rockfall was limited in the previous study. Our work revealed

that the friction might gradually lost its effects on the rolling velocity with increasing slope gradient and the effects would be little when the slope gradient reached 30°.

The rockfall velocity was essential in the assessment and preventive design of the rockfall hazard. After identifying the impact direction, the rockfall mass, action time et al., the impact energy of the rockfall could be calculated. The basic velocity model is $v = \sqrt{2gh}$ where v is velocity; g is acceleration due to gravity; h is fall height. This formula was used for calculating the velocity of a falling rock. With analogous expression for the rockfall velocity, another empirical formula was denoted as:

$$v = a\sqrt{2gh} \tag{8}$$

where a is velocity survival coefficient (Ma et al. 2011). In this study, a simple model for rockfall rolling velocity estimating was proposed, but the rotational component of the rockfall had been neglected for the limitation of test equipment. According to Spadari et al. (2011), the rotational energy represented about 15% of the total energy. So the neglect could be acceptable. In order to verify the applicability of our results and the proposed model, the field tests were conducted. As shown in Figure 13, there were both positive and negative errors in the column of segment C-D while the errors were all positive in the column of segment B-D and A-D indicating that the estimating value was larger than the testing value. From the field tests, it could be reasonably inferred that the rock blocks lost a portion of energy at the point C that resulted in reducing rolling velocity. The energy loss at the point C was ignored in the proposed model. On the other hand, our laboratory study focused on the rolling motion behavior of block on the gentle slope. However, the gradient of the upper segment was steeper than that of the lower segment and laboratory slope which might trigger a transformation of the rock block motion. So, the deviation was significantly affected by the change of gradient. For segment A-D and B-D, the velocity at the point C should be discounted due to energy loss. If the data in these two columns multiply by 0.7 and 0.95 respectively, they would lie under the 10% error boundary (Figure 14). To

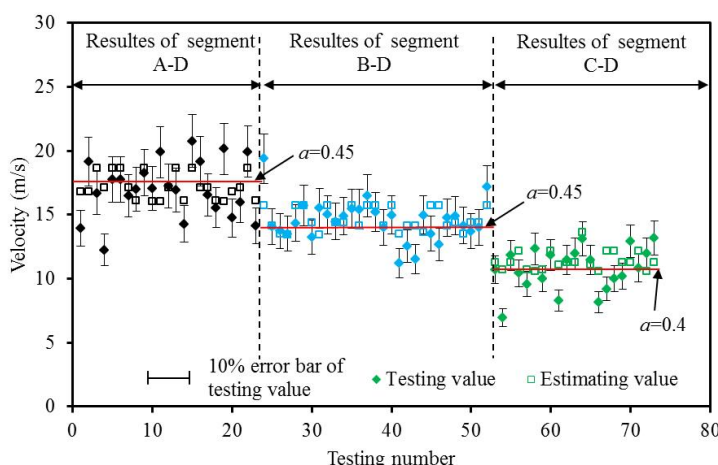


Figure 14 Comparison between the field data with 10% error line and the modified estimating value.

further examine the applicability of our model, the velocity loss due to the variance of gradient needed to be considered independently in the future. If $a = 0.45, 0.45$ and 0.55 , the velocities calculated from Eq.(8) accords with the average value of the testing data. The errors of Eq.(8) were larger than 20%.

The other limitation was the scale effect in our laboratory tests. For rockfall tests the geometrical scale is $\zeta = l / L$, where l is the size of rockfall blocks in the laboratory or the slope model length, and L is the size of rocks in the field or the prototype length. The velocity in the model was ζ^2 times that of the situ. The mass of the block was ζ^3 times that of the situ. The transport time in the model was $\zeta^{1/2}$ times the actual time. The modulus of elasticity of the model was ζ times that of the polytypic. For a laboratory model scaled ζ times, the dimension of the block could be easily adjusted. Because the prototype was much more complicated than the laboratory conditions, some of the other similarity requirements were not easily satisfied simultaneously in the laboratory tests (Chau et al. 2002). Despite the presence of scale effect, the proposed model could provide a first order approximation for the rockfall rolling velocity on a gentle slope. Additionally, data from real events were necessary for further validation and improvement of the proposed model.

6 Conclusions

The influences of the slope surface material, block shape, slope gradient and block mass on the

rockfall rolling motion were analyzed using the orthogonal test method in laboratory. The results showed that the slope surface material, block shape, and slope gradient had significant effects on the rolling motion. The importance of the factors was slope surface material > slope gradient > block shape > block mass. The effect of the slope gradient on the rockfall rolling velocity relied largely on the slope surface condition. The block shape form has little effect on the rockfall rolling velocity when the slope gradient was larger than the critical value. Based on the testing data in the laboratory, a rolling velocity model of the rockfall was proposed.

The model was validated using 73 field tests under straight gentle slope condition. To further examine the applicability of the proposed model, velocity loss due to variance of gradient need to be considered independently in the future.

Acknowledgments

This study was partially supported by the National Science Foundation of China (Grant No. 41572302) and the Funds for Creative Research Groups of China (Grant No. 41521002).

References

- Abellán A, Vilaplana JM, Martínez J (2006) Application of a long-range terrestrial laser scanner to a detailed rockfall study at Vall de Núria (Eastern Pyrenees, Spain). *Engineering Geology* 88(3-4): 136-148. DOI: [10.1016/j.enggeo.2006.09.012](https://doi.org/10.1016/j.enggeo.2006.09.012)
- Apostolou E, Agioutantis Z, Steiakakis C (2015) Integrated evaluation of rockfall triggering mechanism for road monitoring. *Engineering geology for society and territory - volume 2: Landslide processes*, Springer International Publishing, Cham, pp 1975-1978
- Asteriou P, Saroglou H, Tsiambaos G (2012) Geotechnical and kinematic parameters affecting the coefficients of restitution for rock fall analysis. *International Journal of Rock Mechanics and Mining Sciences* 54: 103-113. DOI: [10.1016/j.ijrmms.2012.05.029](https://doi.org/10.1016/j.ijrmms.2012.05.029)
- Asteriou P, Tsiambaos G (2016) Empirical model for predicting rockfall trajectory direction. *Rock Mechanics and Rock Engineering* 49(3): 927-941. DOI: [10.1007/s00603-015-0798-7](https://doi.org/10.1007/s00603-015-0798-7)
- Azzoni A, de Freitas MH (1995) Experimentally gained parameters, decisive for rock fall analysis. *Rock Mechanics and Rock Engineering* 28(2): 111-124. DOI: [10.1007/BF01020064](https://doi.org/10.1007/BF01020064)
- Basson FRP (2012) Rigid body dynamics for rock fall trajectory simulation. 46th US Rock Mechanics/Geomechanics Symposium, American Rock Mechanics Association
- Bourrier F, Berger F, Tardif P, et al. (2012) Rockfall rebound: Comparison of detailed field experiments and alternative modelling approaches. *Earth Surface Processes and Landforms* 37(6): 656-665. DOI: [10.1002/esp.3202](https://doi.org/10.1002/esp.3202)
- Bozzolo D, Pamini R (1986) Simulation of rock falls down a valley side. *Acta Mechanica* 63(1-4): 113-130. DOI: [10.1007/BF01182543](https://doi.org/10.1007/BF01182543)
- Chang YL, Chen CY, Xiao AY (2011) Non-circular rock-fall motion behavior modeling by the eccentric circle model. *Rock Mechanics and Rock Engineering* 44(4): 469-482. DOI: [10.1007/s00603-010-0124-3](https://doi.org/10.1007/s00603-010-0124-3)
- Chau KT, Wong RHC, Liu J, et al. (1999) Shape effects on the coefficient of restitution during rockfall impacts, in: 9th International Congress on Rock Mechanics, Paris, France pp 541-544.
- Chau KT, Wong RHC, Wu JJ (2002). Coefficient of restitution and rotational motions of rockfall impacts. *International Journal of Rock Mechanics and Mining Sciences* 39: 69-77. DOI: [10.1016/S1365-1609\(02\)00016-3](https://doi.org/10.1016/S1365-1609(02)00016-3)
- Chau TK, Wong CRH, Liu J, et al. (2003) Rockfall hazard analysis for hong kong based on rockfall inventory. *Rock Mechanics and Rock Engineering* 36(5): 383-408. DOI: [10.1007/s00603-002-0035-z](https://doi.org/10.1007/s00603-002-0035-z)
- Chen H, Chen RH, Huang TH (1994): An application of an analytical model to a slope subject to rockfall. *Bulletin of the Association of Engineering Geologists* 31(4): 447-458. DOI: [10.2113/gsegeosci.xxxi.4.447](https://doi.org/10.2113/gsegeosci.xxxi.4.447)
- Chen GQ, Zheng L, Zhang YB, et al. (2013) Numerical simulation in rockfall analysis: A close comparison of 2-D and 3-D DDA. *Rock Mechanics and Rock Engineering* 46(3): 527-541. DOI: [10.1007/s00603-012-0360-9](https://doi.org/10.1007/s00603-012-0360-9)
- Copons R, Vilaplana JM, Linares R (2009) Rockfall travel distance analysis by using empirical models (Sola d'Andorra la Vella, Central Pyrenees). *Natural Hazards & Earth System Sciences* 9(6): 2107-2118. DOI: [10.5194/nhess-9-2107-2009](https://doi.org/10.5194/nhess-9-2107-2009)
- Crosta GB, Agliardi F (2004) Parametric evaluation of 3D dispersion of rockfall trajectories. *Natural Hazards and Earth System Science* 4(4): 583-598. DOI: [10.5194/nhess-4-583-2004](https://doi.org/10.5194/nhess-4-583-2004)
- Dorren LK (2003) A review of rockfall mechanics and modelling approaches. *Progress in Physical Geography* 27(1): 69-87. DOI: [10.1191/0309133303pp359ra](https://doi.org/10.1191/0309133303pp359ra)
- Dorren LKA, Seijmonsbergen AC (2003) Comparison of three GIS-based models for predicting rockfall runout zones at a regional scale. *Geomorphology* 56(1-2): 49-64. DOI: [10.1016/S0169-555X\(03\)00045-X](https://doi.org/10.1016/S0169-555X(03)00045-X)
- Dorren LKA, Berger F, Putters US (2006) Real-size experiments and 3-D simulation of rockfall on forested and non-forested slopes. *Natural Hazards and Earth System Science* 6(1): 145-153. DOI: [10.5194/nhess-6-145-2006](https://doi.org/10.5194/nhess-6-145-2006)
- Evans SG, Hungr O (1993) The assessment of rockfall hazard at the base of talus slopes. *Canadian Geotechnical Journal* 30: 620-636. DOI: [10.1139/t93-054](https://doi.org/10.1139/t93-054)
- Ferrari F, Thoeni K, Giacomini A, et al. (2016) A rapid approach to estimate the rockfall energies and distances at the base of rock cliffs. *Georisk: Assessment and Management of Risk for Engineered Systems and Geohazards* 10(3): 179-199. DOI: [10.1080/17499518.2016.1139729](https://doi.org/10.1080/17499518.2016.1139729)
- Fityus SG, Giacomini A, Buzzi O (2013) The significance of geology for the morphology of potentially unstable rocks. *Engineering Geology* 162: 43-52. DOI: [10.1016/j.enggeo.2013.05.007](https://doi.org/10.1016/j.enggeo.2013.05.007)
- Fityus SG, Giacomini A, Thoeni K (2015) The Influence of Shape on the Inherent Rolling Potential of Loose Rocks. *Engineering Geology for Society and Territory* 2: 2045-2048. DOI: [10.1007/978-3-319-09057-3_364](https://doi.org/10.1007/978-3-319-09057-3_364)
- Fan XY, Tian SJ, Zhang YY (2016) Mass-front velocity of dry granular flows influenced by the angle of the slope to the runout plane and particle size gradation. *Journal of Mountain Science* 13(2): 234-245. DOI: [10.1007/s11629-014-3396-3](https://doi.org/10.1007/s11629-014-3396-3)

- Giani G, Giacomini A, Migliazza M, et al. (2004) Experimental and Theoretical Studies to Improve Rock Fall Analysis and Protection Work Design. *Rock Mechanics and Rock Engineering* 37(5): 369-389. DOI: [10.1007/s00603-004-0027-2](https://doi.org/10.1007/s00603-004-0027-2)
- Glover J, Schweizer A, Christen M, et al. (2012) Numerical investigation of the influence of rock shape on rockfall trajectory. *General Assembly Conference Abstracts* 14: EGU2012-11022-1
- Guzzetti F, Reichenbach P, Wieczorek GF (2003) Rockfall hazard and risk assessment in the Yosemite valley, California, USA. *Nat Hazard Earth Sys* 3(6): 491-503. DOI: [10.5194/nhess-3-491-2003](https://doi.org/10.5194/nhess-3-491-2003)
- Huang RQ, Liu WH, Zhou JP, et al. (2007) Rolling tests on movement characteristics of rock block. *Chines Journal of Geotechnical Engineering* 29: 1296-1302. (In Chinese)
- Jaboyedoff M, Baillifard F, Bardou E, et al. (2004) The effect of weathering on alpine rock instability. *Quarterly Journal of Engineering Geology and Hydrogeology* 37(2): 95-103. DOI: [10.1144/1470-9236/03-046](https://doi.org/10.1144/1470-9236/03-046)
- Jaboyedoff M, Dudt JP, Labiouse V (2005). An attempt to refine rockfall hazard zoning based on the kinetic energy, frequency and fragmentation degree. *Natural Hazards and Earth System Science* 5(5): 621-632. DOI: [10.5194/nhess-5-621-2005](https://doi.org/10.5194/nhess-5-621-2005)
- Jomelli V, Francou B (2000) Comparing the characteristics of rockfall talus and snow avalanche landforms in an Alpine environment using a new methodological approach: Massif des Ecrins, French Alps. *Geomorphology* 35(3-4): 181-192. DOI: [10.1016/S0169-555X\(00\)00035-0](https://doi.org/10.1016/S0169-555X(00)00035-0)
- Kirkby MJ, Satham I (1975) Surface stone movement and scree formation. *Journal of Geology* 83(3): 349-362. DOI: [10.1086/628097](https://doi.org/10.1086/628097)
- Labiouse V, Heidenreich B (2009) Half-scale experimental study of rockfall impacts on sandy slopes. *Natural Hazards and Earth System Science* 9(6): 1981-1993. DOI: [10.5194/nhess-9-1981-2009](https://doi.org/10.5194/nhess-9-1981-2009)
- Lan HX, Martin CD, Lim CH (2007) Rockfall analyst: A Gis extension for three-dimensional and spatially distributed rockfall hazard modeling. *Computers & Geosciences* 33(2): 262-279. DOI: [10.1016/j.cageo.2006.05.013](https://doi.org/10.1016/j.cageo.2006.05.013)
- Lan HX, Martin CD, Zhou CH, et al. (2010) Rockfall hazard analysis using Lidar and spatial modeling. *Geomorphology* 118(1-2): 213-223. DOI: [10.1016/j.geomorph.2010.01.002](https://doi.org/10.1016/j.geomorph.2010.01.002)
- Leine RI, Schweizer A, Christen M, et al. (2014) Simulation of rockfall trajectories with consideration of rock shape. =Multibody System Dynamics 32(2): 241-271. DOI: [10.1007/s11044-013-9393-4](https://doi.org/10.1007/s11044-013-9393-4)
- Ma GC, Matsuyama H, Nishiyama S, et al. (2011) Practical studies on rockfall simulation by DDA. *Journal of Rock Mechanics and Geotechnical Engineering* 3(1): 57-63. DOI: [10.3724/SP.J.1235.2011.00057](https://doi.org/10.3724/SP.J.1235.2011.00057)
- Okura Y, Kitahara H, Sammori T, et al. (2000). The effects of rockfall volume on runout distance. *Engineering Geology* 58(2): 109-124. DOI: [10.1016/S0013-7952\(00\)00049-1](https://doi.org/10.1016/S0013-7952(00)00049-1)
- Paronuzzi P (2009) Rockfall-induced block propagation on a soil slope, northern Italy. *Environmental geology* 58: 1451-1466. DOI: [10.1007/s00254-008-1648-7](https://doi.org/10.1007/s00254-008-1648-7)
- Pei XJ, Huang RQ, Pei Z, et al. (2011) Analysis on the movement characteristics of rolling rock on slope caused by intensities earthquake *Journal of Engineering Geology* 19(4): 498-504. (In Chinese)
- Pei XJ, Liu Y, Wang DP (2016) Study on the Energy Dissipation of Sandy Soil Cushions on the Rock-shed Under Rockfall Impact Load *Journal of Sichuan University (Engineering Science Edition)* 48(1): 15-22. (In Chinese)
- Pellicani R, Spilotro G, Van Westen CJ (2016) Rockfall trajectory modeling combined with heuristic analysis for assessing the rockfall hazard along the Maratea SS18 coastal road (Basilicata, Southern Italy). *Landslides* 13(5): 985-1003. DOI: [10.1007/s10346-015-0665-3](https://doi.org/10.1007/s10346-015-0665-3)
- Perret S, Dolf F, Kienholz H (2004) Rockfalls into forests: Analysis and simulation of rockfall trajectories — considerations with respect to mountainous forests in Switzerland. *Landslides* 1(2): 123-130. DOI: [10.1007/s10346-004-0014-4](https://doi.org/10.1007/s10346-004-0014-4)
- Piacentini D, Soldati M (2008) Application of empiric models for the analysis of rock-fall runout at a regional scale in mountain areas: Examples from the Dolomites and the northern Apennines (Italy). *Geografia Fisica E Dinamica Quaternaria* 31(2): 215-223.
- Ritchie AM (1963) Evaluation of rock fall, its control. *HRB, Highway Research Record* (17): 13-28.
- Saroglou H, Marinos V, Marinos P, et al. (2012) Rockfall hazard and risk assessment: An example from a high promontory at the historical site of Monemvasia, Greece. *Natural Hazards and Earth System Sciences* 12(6): 1823-1836. DOI: [10.5194/nhess-12-1823-2012](https://doi.org/10.5194/nhess-12-1823-2012)
- Sass O, Krautblatter M (2007) Debris flow-dominated and rockfall-dominated talus slopes: Genetic models derived from GPR measurements. *Geomorphology* 86(1-2): 176-192. DOI: [10.1016/j.geomorph.2006.08.012](https://doi.org/10.1016/j.geomorph.2006.08.012)
- Selby MJ (1982) *Hillslope materials and processes*. New York: Oxford University Press
- Spadari M, Giacomini A, Buzzi O, et al. (2012). In situ rockfall testing in New South Wales Australia. *International Journal of Rock Mechanics and Mining Sciences* 49: 84-93. DOI: [10.1016/j.ijrmms.2011.11.013](https://doi.org/10.1016/j.ijrmms.2011.11.013)
- Thoeni K, Giacomini A, Lambert C, et al. (2014) A 3D discrete element modelling approach for rockfall analysis with drapery systems. *International Journal of Rock Mechanics and Mining Sciences* 68: 107-119. DOI: [10.1016/j.ijrmms.2014.02.008](https://doi.org/10.1016/j.ijrmms.2014.02.008)
- Vijayakumar S, Yacoub T, Curran JH (2011) On the effect of rock size and shape in rockfall analyses. *proceedings of the US rock mechanics symposium (ARMA)* San Francisco CA, USA
- Volkwein A, Schellenberg K, Labiouse V, et al. (2011) Rockfall characterisation and structural protection—a review. *Natural Hazards and Earth System Sciences* 11(9): 2617-2651. DOI: [10.5194/nhess-11-2617-2011](https://doi.org/10.5194/nhess-11-2617-2011)
- Wang Y, Tonon F (2011) Discrete element modeling of rock fragmentation upon impact in rock fall analysis. *Rock mechanics and rock engineering* 44(1): 23-35. DOI: [10.1007/s00603-010-0110-9](https://doi.org/10.1007/s00603-010-0110-9)
- Zvelebil J, Moser M (2001) Monitoring based time-prediction of rock falls: three case-histories. *Physics and Chemistry of the Earth (B)* 26(2): 159-167. DOI: [10.1016/S1464-1909\(00\)00234-3](https://doi.org/10.1016/S1464-1909(00)00234-3)